Mitigation of PM Eddy Current Losses Using Offset Windings in Coreless AFPM Machines

Matin Vatani
SPARK Lab, Pigman Eng. College
University of Kentucky
Lexington, KY, USA
matin.vatani@uky.edu

Diego A. Lopez Guerrero
SPARK Lab, Pigman Eng. College
University of Kentucky
Lexington, KY, USA
diegolopezg@uky.edu

John F. Eastham
Dept. of Electronic & Electrical Eng.
University of Bath
Claverton Down, Bath, UK
jfeastham@aol.com

Dan M. Ionel
SPARK Lab, Pigman Eng. College
University of Kentucky
Lexington, KY, USA
dan.ionel@ieee.org

***Abstract*—Permanent magnet eddy current losses can become substantial in coreless stator axial flux permanent magnet (AFPM) machines operating at high speeds and under high electric loading, potentially leading to elevated temperatures and an increased risk of demagnetization. This paper investigates the origins of these losses through a detailed harmonic analysis of the winding factor and introduces a mitigation strategy. The proposed method utilizes two-layer offset windings, effectively minimizing undesirable armature flux harmonics through harmonic interaction between the offset layers. Two cases are studied: one in which each stator layer is connected to a separate inverter and another in which both layers are connected in parallel and driven by a single inverter. Three-dimensional finite element analysis (FEA) results demonstrate a significant reduction in PM eddy current losses achieved using this approach. Further PM eddy current loss mitigation is explored through the combined use of winding offset and segmented magnets, demonstrating that these losses are reduced by 95% compared to the original design.**

***Index Terms*—Eddy current, permanent magnet loss, rotor loss, axial flux, coreless stator, magnet segmentation.**

I. Introduction

Axial flux PM machines are widely recognized for their high torque density and axially compact design, making them ideal for applications requiring compact form factor [1–3]. They allow for the use of higher pole numbers compared to their radial flux counterparts [4], which can lead to a higher power-to-mass ratio, as demonstrated in [5]. Due to improved accessibility to the stator windings, AFPM machines enable the implementation of advanced direct cooling methods, as presented in [6, 7], making them more suitable for applications that demand ultra-efficient electric motors.

Coreless stator AFPM machines can achieve higher power-to-mass ratios and efficiencies than conventional AFPM machines, primarily due to the elimination of stator cores and their associated losses [8]. Although the absence of a core exposes the winding conductors directly to the varying rotor magnetic field, inducing eddy current losses on the conductors, this can be effectively mitigated through the use of Litz wire or printed circuit boards (PCBs) with conductor transposition, as demonstrated in [9]. Coreless designs offer improved access to the windings, facilitating the implementation of more effective cooling solutions, such as those shown in [10], thereby enabling higher current loading capabilities.

Magnet eddy current loss can be a significant source of loss in PM electric machines, particularly in high-speed applications, as it increases rapidly with rotational speed. These losses raise the temperature of the magnets, negatively impacting electromagnetic performance and potentially leading to irreversible demagnetization [11, 12]. In coreless stator AFPM machines, PM eddy current losses are typically neglected because of the typically low armature reaction [13]. This paper demonstrates that PM eddy current losses can become the dominant loss component in coreless AFPM machines when operating at high speed and high current densities, which are typical conditions for electric aircraft propulsion.

The rotor configuration also influences PM eddy current losses. For example, in surface-mounted rotors, the pole arc is a key design parameter that affects these losses. While a larger pole arc can increase torque output, it also extends the eddy current path within the magnets, leading to greater associated losses. In this context, PM eddy current losses can be more severe in Halbach array rotors, where the entire rotor surface is covered with magnets. Although Halbach array PM rotors offer higher specific torque density than surface-mounted PM rotors of the same size, they require a larger volume of magnet material, which contributes to elevated eddy current losses.

While conventional methods, such as magnet segmentation, are commonly employed to mitigate these losses, they often fall short in effectiveness or introduce significant manufacturing complexities and precision issues. When eddy current losses are substantial, very small magnet segments are required to mitigate them. This can be impractical to implement, particularly in Halbach array PM rotors, where the assembly process is already complex.

This paper presents a practical and highly effective solution for mitigating PM eddy current losses in coreless stator AFPM

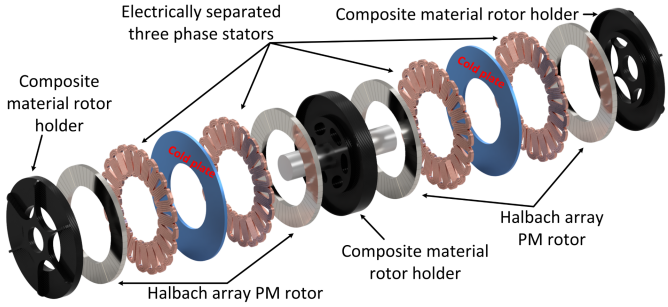

Figure 1. Exploded view of the dual-stage coreless stator AFPM machine, featuring Halbach array rotors, concentrated stator windings, and an integrated cooling system.

machines. This paper is structured into six sections. Section II details the coreless AFPM machine topology for electric aircraft propulsion. Section III presents the problem formulation of PM eddy current losses. Section IV describes the proposed offset winding approach for PM eddy current loss mitigation. Section V discusses the effect of magnet segmentation, and Section VI presents the conclusions.

II. Coreless Axial Flux PM Machine Topology

The proposed electric motor for aircraft propulsion comprises two identical stages of coreless stator AFPM machines, as shown in Fig. 1 [14]. These stages are magnetically and electrically isolated while sharing a common mechanical assembly mounted on a single shaft. Each stage includes a double-sided Halbach array PM rotor and two three-phase stators, with the multiphysics design methodology detailed in [15]. The stators are powered by five-level active neutral-point clamped (5L-ANPC) inverters, as described in [16]. Within each stage, the stators can either be connected in parallel and driven by a single inverter or powered independently by two separate inverters to enhance system reliability.

The double-stage motor delivers a maximum power of 2 MW at 3,500 rpm during take-off, with both stages operating simultaneously and each generating 1 MW. During the cruise, the power requirement is reduced to half, allowing for flexible operation: either both stages can operate at half power, or one stage can be deactivated while the other runs at full load. This redundancy significantly enhances fault tolerance. If a fault occurs in one stage, the remaining stage can maintain cruise and landing operations, ensuring continued functionality under emergency conditions.

The thermal management system incorporates two cold plates positioned between the stators in each stage.These plates employ liquid hydrogen cooling at cryogenic temperatures, enabling the motor to achieve a peak efficiency exceeding 99% at -140°C. The cold plates are made of aluminum nitride, chosen for their excellent thermal conductivity and poor electrical and magnetic properties, minimizing magnetic interference while enhancing heat dissipation.

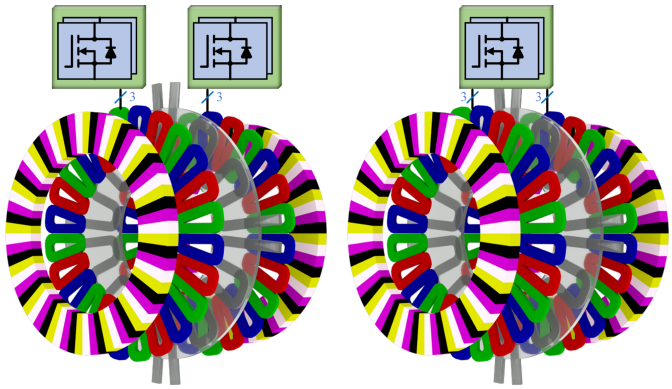

(a) (b)

Figure 2. Possible stator and inverter configurations for one stage of the proposed coreless AFPM machine: (a) two stators connected to separate inverters (electrically independent stators), and (b) stators connected in parallel and driven by a single inverter.

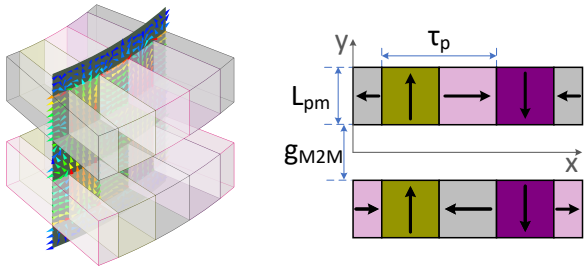

(a) (b)

Figure 3. Two-pole section of the double-sided Halbach array rotor: (a) three-dimensional flux density distribution on a plane at the average radius, and (b) equivalent two-dimensional view of an unrolled plane at an arbitrary radius.

III. Magnet Eddy Current Losses Problem Formulation

Neodymium Iron Boron (NdFeB) PMs exhibit high electrical conductivity compared to other PM materials [17, 18], making them susceptible to high eddy current losses. At high electric loading or speeds, non-torque-producing armature flux harmonics can induce eddy currents in the magnets, leading to increased losses, elevated temperatures, and a heightened risk of demagnetization.

In conventional coreless stator AFPM machines, armature flux and its harmonics are typically minimal, allowing eddy current losses in the magnets to be neglected. This study demonstrates that in high-performance coreless stator machines, such as the proposed design for electric aircraft propulsion, significant eddy current losses can occur due to elevated speeds and current loading. This section analyzes the sources of eddy currents in the PMs by identifying non-torque-producing harmonics generated by the stator. Rotor harmonics all travel at rotor speed and cannot induce eddy currents in the PMs, as stated later in the paper.

The proposed machine features a double-sided Halbach array rotor with four PMs per wavelength, forming a 90-degree Halbach array. Figure 3a illustrates the flux density

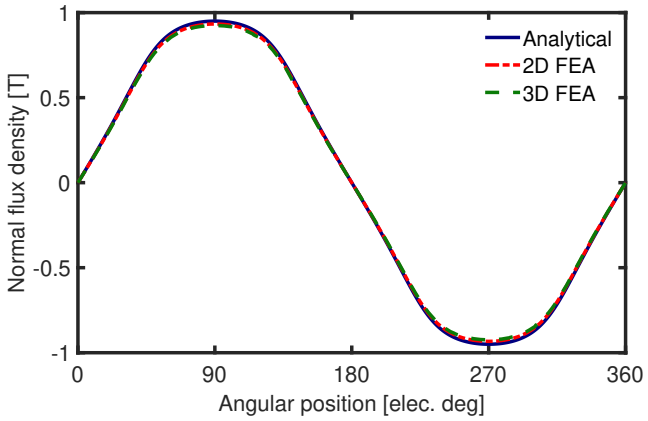

(a)

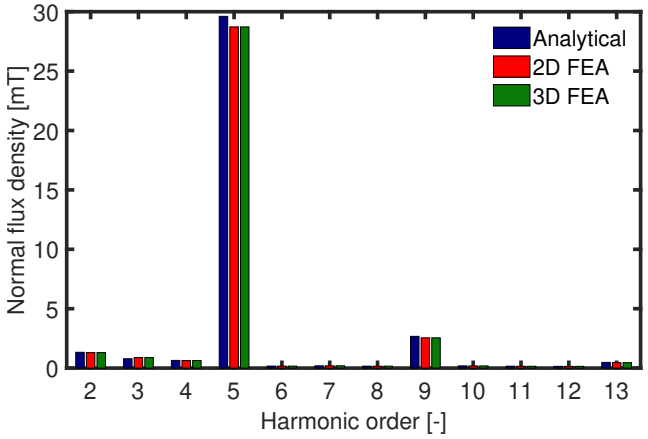

(b)

Figure 4. Normal flux density at the midpoint of the magnet-to-magnet gap and average radius, computed using analytical equations and 2D/3D finite element analysis (FEA): (a) flux density waveforms, and (b) corresponding harmonic spectra with the fundamental component of 0.97 T excluded.

vector distribution on the rotor surface at no-load conditions, measured at the average diameter. By unrolling that surface, an equivalent linear machine model is created, enabling two-dimensional analysis, as illustrated in Fig. 3b. The normal component of the flux density for a linear double-sided Halbach array can be calculated using [19]:

$$B_n = 2B_r \sum_{\nu=0}^{\infty} \frac{\sin(\epsilon n\pi/m)}{n\pi/m}\left[1-\exp\left(\frac{-n\pi L_{pm}}{\tau_p}\right)\right] \exp\left(\frac{-n\pi g_{M2M}}{2\tau_p}\right)\cosh\left(\frac{n\pi y}{\tau_p}\right)\sin\left(\frac{n\pi x}{\tau_p}\right), \quad (1)$$

where B_r represents the remanence of the PMs, and ϵ is a constant, typically set to one. The term $n = 1 + m\nu$, where m denotes the number of PMs per wavelength, and ν represents the harmonic order. L_{PM} is the length of the PM, τ_p is the pole pitch width, and g_{M2M} is the magnet-to-magnet gap. The coordinates y and x correspond to the positions in the Y and X directions, respectively, as defined in Fig. 3b.

According to Equation 1, a Halbach array with four PMs per wavelength generates 5^{th}, 9^{th}, 13^{th}, 17^{th}, and higher-order

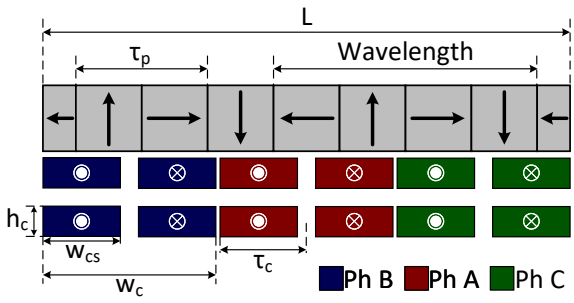

Figure 5. Geometric parameters of the four-pole, three-coil configuration with a double-layer stator.

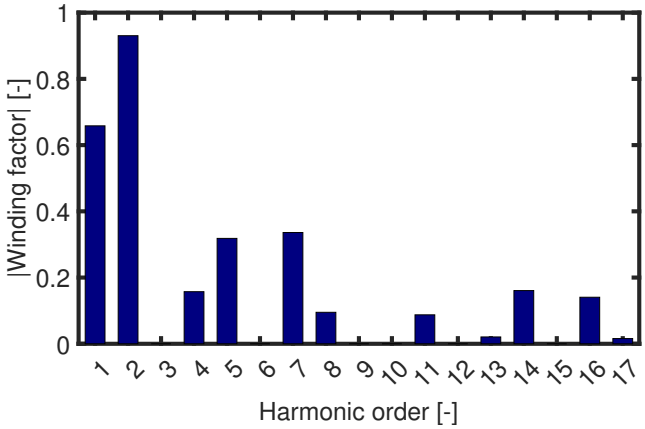

Figure 6. Harmonic content of the winding factor for $K = 0.6$, where the second harmonic contributes to torque production, and other harmonics cause minor torque ripple and magnet eddy current losses.

spatial harmonics. The flux density at the midpoint of the air-gap, $y = 0$, was computed using an analytical approach and 2/3D FEA at the average radius. The flux density curves are presented in Fig. 4a and the corresponding harmonic spectrum is shown in Fig. 4b. The fundamental and harmonic components of the rotor flux density all rotate at the synchronous speed, with only the fundamental component contributing to torque production. The higher-order rotor harmonics are not synchronized with the armature field harmonics and do not contribute to torque generation.

To determine the harmonic spectrum of the armature flux, the winding factor is calculated for the four-pole, three-coil configuration used in the proposed machine. This analysis identifies non-torque-producing harmonics that induce eddy currents in the PMs. The total winding factor is the product of the conductor distribution factor, K_T, pitch factor, K_p, and coil group factor, K_g, and can be calculated from:

$$K_T = \frac{2N_c}{K\pi\nu}\sin\left(\frac{K\pi\nu}{2N_c}\right), \quad (2)$$

$$K_p = \sin\left(\frac{\nu\pi\,(2-K)}{2N_c}\right), \quad (3)$$

where $N_c = 3$ represents the number of coils, ν denotes the harmonic order, and K is the ratio of the coil side width to

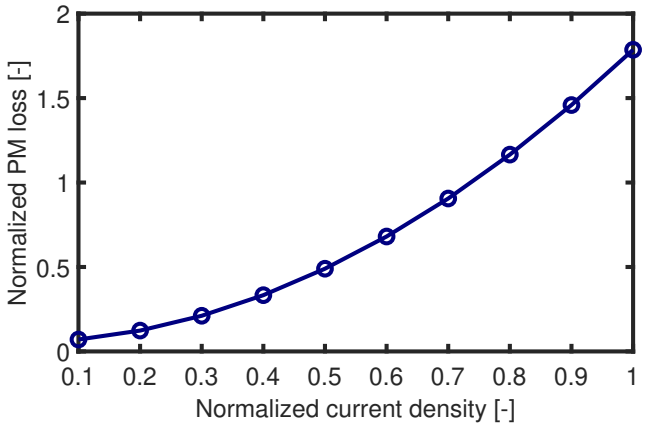

Figure 7. Effect of stator current density on PM eddy current loss, with current density normalized to its rated value and PM eddy current loss normalized to the Joule loss.

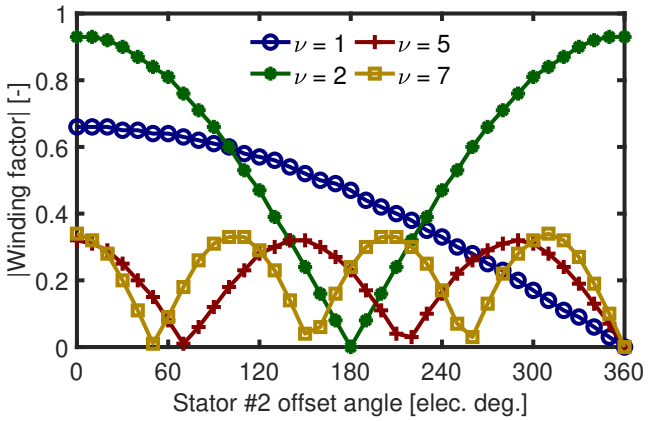

Figure 9. Overall winding factor of the double-layer stator as a function of the shift angle between layers, assuming both stators are connected in parallel and fed by a single inverter with pure sinusoidal current excitation.

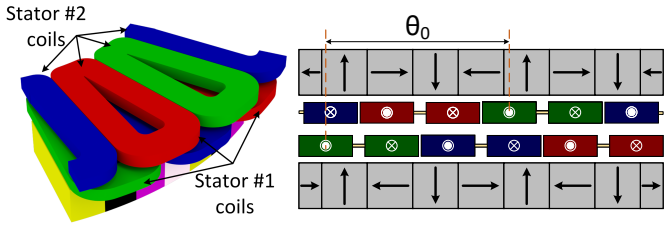

Figure 8. Proposed two-layer offset winding configuration with a 360° electrical offset for harmonic suppression and reduction of PM eddy current losses, shown in (a) a 3D representation and (b) a 2D schematic.

the coil pitch, as defined in Fig. 5, depending on the radius at which the calculation is performed. The coil group factor is equal to one for the 4/3 pole-to-coil combination.

The harmonic spectrum of the winding factor is calculated and shown in Fig. 6, revealing significant non-torque-producing harmonics. Except for the second harmonic, other harmonics do not contribute to torque generation but can induce eddy currents in the PMs. The PM eddy current losses for one stage of the proposed machine were evaluated using 3D FEA under varying current densities, with the results presented in Fig. 7. The PM eddy current losses are normalized relative to the copper losses of the machine at rated conditions, while the current density is normalized based on its maximum value at rated operation. The results indicate that PM eddy current losses increase with higher current loading. At rated conditions, these losses become the dominant losses, exceeding copper losses by more than 50%.

IV. Mitigation of Magnet Eddy Current Losses Using Offset Windings

In order to mitigate eddy current losses in the PMs, non-torque-producing armature harmonics must be suppressed [20]. This section proposes a double-layer offset winding configuration to achieve this objective. The concept is illustrated in both 3D and 2D views in Fig. 8, where one winding layer is angularly shifted relative to the other. The optimal offset angle for minimizing PM eddy current losses is determined for the case where both winding layers are connected in parallel and powered by a single inverter, as well as for the case where each layer is driven independently by a separate inverter.

A. Parallel-Connected Stators with a Single Inverter

For this case, if the winding factor of the non-offset winding is denoted by $\overline{N_t}$, the total winding factor when one layer is offset by θ_0 electrical degrees can be expressed as:

$$\overline{N_{t_{offset}}} = \frac{\overline{N_t}\left(1+e^{-\frac{2j\theta_0\nu}{P}}\right)}{2} = \overline{N_t}e^{\frac{-j\theta_0\nu}{P}}\cos\left(\frac{\theta_0\nu}{P}\right), \quad (4)$$

and if the stator is rotated in the reverse direction:

$$\overline{N_{t_{offset}}} = \frac{\overline{N_t}\left(1-e^{-\frac{2j\theta_0\nu}{P}}\right)}{2} = \overline{N_t}e^{\frac{-j\theta_0\nu}{P}}\sin\left(\frac{\theta_0\nu}{P}\right). \quad (5)$$

where P is the base pole number, which is 4 in this study, as the proposed coreless AFPM machine employs a 4/3 pole-to-coil combination. The amplitude of the winding factor for the two-layer stator, where one layer is offset, is modified by a factor of $|\cos\left(\frac{\theta_0\nu}{P}\right)|$. If the offset direction is reversed, the amplitude is instead modified by $|\sin\left(\frac{\theta_0\nu}{P}\right)|$. It is important to note that θ_0 in 4 and 5 is expressed in electrical degrees.

In the case study presented in this paper, the coreless AFPM machine employs a base pole-to-coil combination of 4/3, resulting in the second harmonic of the armature field contributing to torque production, while the remaining harmonics induce eddy currents in the PMs. To minimize these losses, the non-torque-producing harmonics with the largest amplitude must be suppressed. Therefore, as shown in Fig. 6, the first harmonic should be eliminated, which requires $\cos\left(\frac{\theta_0}{4}\right) = 0 \Rightarrow \theta_0 = 360$ electrical degrees.

The winding factor for the two-layer offset winding at various offset angles for the 1st, 2nd, 5th, and 7th harmonics—identified as having higher amplitudes than other harmonic orders—is presented in Fig. 8. To maintain the rated torque, the offset angle should be chosen to maximize the

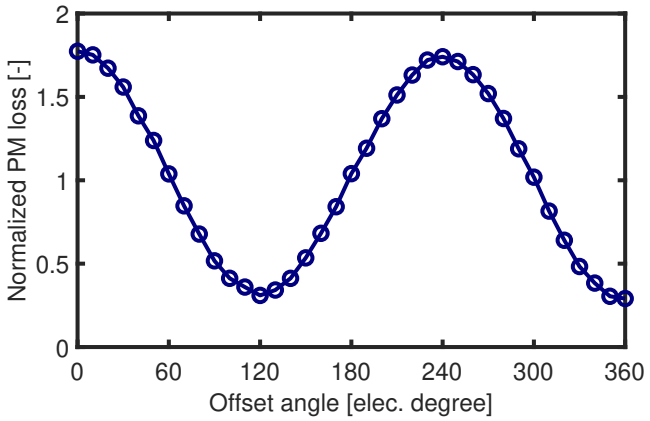

Figure 10. Normalized PM eddy current loss at rated stator current density as a function of the offset angle between layers, assuming each layer is driven by a separate inverter with pure sinusoidal excitation.

winding factor of the second harmonic, which contributes to torque production, while minimizing the winding factors of non-torque-producing harmonics to reduce PM eddy current losses. An offset angle of 360 electrical degrees effectively suppresses the dominant non-torque-producing harmonics and maximizes the second harmonic component. The PM eddy current loss, calculated with an offset angle of 360 electrical degrees, shows that the rated torque is maintained while the loss is reduced by 85%.

B. Independently-Driven Stators with Separate Inverters

In the second case, the two stators in each stage of the machine are electrically isolated, as they are connected to two separate inverters. This subsection demonstrates that the winding offset remains effective for mitigating PM eddy current losses in this configuration. The optimal offset angle does not follow the same rule as the single-inverter case.

A parametric study was conducted across various offset angles to evaluate their effect on PM eddy current losses. Each stator was supplied with a symmetrical three-phase current, phase-shifted by the corresponding offset angle. The current was injected in alignment with the back electromotive force (B-EMF) of each stator, ensuring that the motor consistently produced rated torque regardless of the offset angle.

The results, presented in Fig. 10, show that the minimum PM eddy current loss occurs at an offset angle of 120 electrical degrees, achieving an 82% reduction compared to the zero-offset case. The variation in PM eddy current loss follows a cosine-like dependence on the offset angle, with a periodicity of 240 electrical degrees.

V. Magnet Segmentation

A common approach to reducing PM eddy current losses involves segmenting the magnets radially in AFPM machines, as for example demonstrated in [21]. While dividing each magnet block into a few segments effectively minimizes losses, excessive segmentation introduces challenges such as assembly complexity and reduced manufacturing precision.

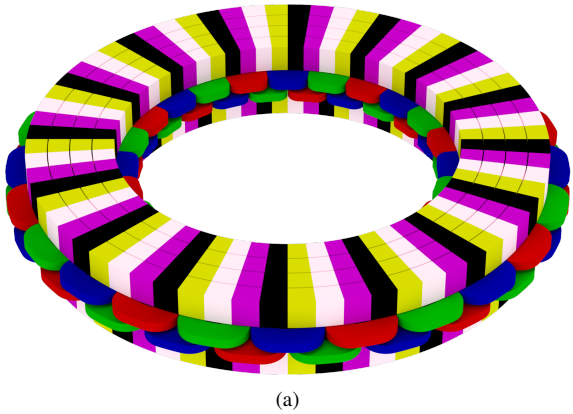

(a)

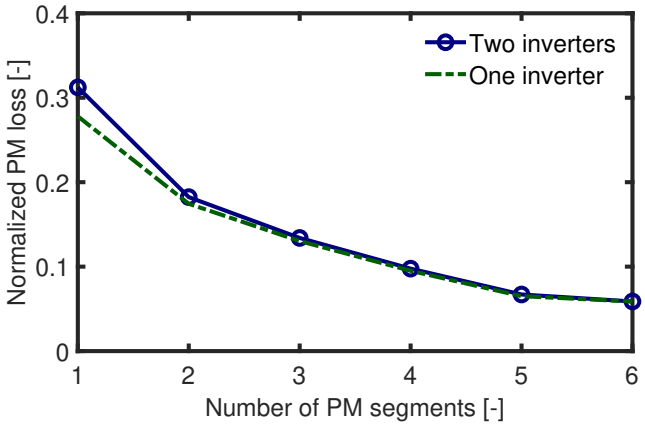

(b)

Figure 11. One stage of the proposed coreless AFPM machine featuring double-layer offset windings and segmented PMs (a) and effect of PM segmentation on PM eddy current losses at rated load for two configurations: parallel-connected windings fed by a single inverter and individually fed windings using separate inverters (b).

Moreover, this approach significantly increases production expenses for cost-sensitive applications.

This paper proposed an offset winding configuration that significantly reduces PM eddy current losses. Further reduction is achievable when this technique is combined with radial segmentation of the magnets. A parametric analysis of PM eddy current losses as a function of the number of magnet segments with the optimal offset angle applied is presented in Fig. 11b. The results show that segmenting the magnets into six radial pieces reduces the PM eddy current losses to less than 0.1 times the copper losses.

Achieving such low PM eddy loss levels with six segments would not be possible without the proposed offset winding approach. It would otherwise require an impractically high number of very thin magnet segments, posing significant manufacturing challenges.

VI. Conclusion

This paper proposed a two-layer offset winding method for mitigating PM eddy current losses in coreless stator AFPM machines. Analytical, 2D, and 3D FEA were conducted to examine the airgap flux density under no-load conditions and

to identify its harmonic distribution. A detailed harmonic analysis of the winding factor for a four-pole, three-coil configuration indicated significant harmonics from non-torque-producing components. It was demonstrated that employing a two-layer winding configuration, with one layer offset relative to the other, effectively minimizes unwanted harmonics. The PM eddy current loss calculations showed an approximately 85% reduction in PM losses using the proposed offset winding. Furthermore, an analysis combining the offset winding method with PM segmentation revealed that the required magnet segments could be substantially reduced, simplifying manufacturing while maintaining performance.

ACKNOWLEDGMENT

The support of the Leverhulme Trust, under their visiting professorship scheme, and of University of Kentucky the L. Stanley Pigman Chair in Power endowment is gratefully acknowledged. Any opinions, findings, and conclusions or recommendations expressed in this material are those of the authors and do not necessarily reflect the views of the sponsoring organizations.

REFERENCES

[1] F. Nishanth, J. Van Verdeghem, and E. L. Severson, "A review of axial flux permanent magnet machine technology," *IEEE Transactions on Industry Applications*, vol. 59, no. 4, pp. 3920–3933, 2023.

[2] M. Aydin, S. Huang, and T. Lipo, "Axial flux permanent magnet disc machines: A review," *Conf. Record of SPEEDAM*, 01 2004.

[3] F. G. Capponi, G. De Donato, and F. Caricchi, "Recent advances in axial-flux permanent-magnet machine technology," *IEEE Transactions on Industry Applications*, vol. 48, no. 6, pp. 2190–2205, 2012.

[4] J. F. Gieras, R.-J. Wang, and M. J. Kamper, *Axial flux permanent magnet brushless machines*. Springer Science & Business Media, 2008.

[5] M. Vatani, J. F. Eastham, and D. M. Ionel, "Multi-disk coreless axial flux permanent magnet synchronous motors with surface PM and Halbach array rotors for electric aircraft propulsion," in *2024 IEEE Energy Conversion Congress and Exposition (ECCE)*. IEEE, 2024, pp. 4986–4992.

[6] R. Camilleri and M. D. McCulloch, "Integrating a heat sink into concentrated wound coils to improve the current density of an axial flux, direct liquid cooled electrical machine with segmented stator," *Energies*, vol. 14, no. 12, p. 3619, 2021.

[7] C. Jenkins, S. Jones-Jackson, I. Zaher, G. Pietrini, R. Rodriguez, J. Cotton, and A. Emadi, "Innovations in axial flux permanent magnet motor thermal management for high power density applications," *IEEE Transactions on Transportation Electrification*, vol. 9, no. 3, pp. 4380–4405, 2023.

[8] M. Vatani, A. Mohammadi, D. Lewis, J. F. Eastham, and D. M. Ionel, "Coreless axial flux Halbach array permanent magnet generator concept for direct-drive wind turbine," in *2023 12th International Conference on Renewable Energy Research and Applications (ICRERA)*. IEEE, 2023, pp. 612–617.

[9] Y. Chulaee, D. Lewis, M. Vatani, J. F. Eastham, and D. M. Ionel, "Torque and power capabilities of coreless axial flux machines with surface PMs and Halbach array rotors," in *2023 IEEE International Electric Machines & Drives Conference (IEMDC)*. IEEE, 2023, pp. 1–6.

[10] M. Vatani, Y. Chulaee, J. F. Eastham, X. Pei, and D. M. Ionel, "Multi-wound axial flux generators with Halbach array rotors," in *2024 IEEE Energy Conversion Congress and Exposition (ECCE)*. IEEE, 2024, pp. 5199–5204.

[11] G. Choi and T. M. Jahns, "Reduction of eddy-current losses in fractional-slot concentrated-winding synchronous PM machines," *IEEE transactions on magnetics*, vol. 52, no. 7, pp. 1–4, 2016.

[12] J. Ma and Z. Zhu, "Magnet eddy current loss reduction in permanent magnet machines," *IEEE Transactions on Industry Applications*, vol. 55, no. 2, pp. 1309–1320, 2018.

[13] J. Santiago, J. Oliveira, J. Lundin, A. Larsson, and H. Bernhoff, "Losses in axial-flux permanent-magnet coreless flywheel energy storage systems," in *2008 18th International Conference on Electrical Machines*. IEEE, 2008, pp. 1–5.

[14] D. D. Lewis, D. R. Stewart, M. Vatani, O. A. Badewa, A. Mohammadi, and D. M. Ionel, "Fault-tolerant topologies with Halbach array and PM-free multi-stage multi-module electric machines for electric aircraft propulsion," in *2024 IEEE Energy Conversion Congress and Exposition (ECCE)*. IEEE, 2024, pp. 2524–2528.

[15] M. Vatani, Y. Chulaee, A. Mohammadi, D. R. Stewart, J. F. Eastham, and D. M. Ionel, "On the optimal design of coreless AFPM machines with Halbach array rotors for electric aircraft propulsion," in *2024 IEEE Transportation Electrification Conference and Expo (ITEC)*. IEEE, 2024, pp. 1–6.

[16] F. Y. Notash, M. Vatani, J. He, and D. M. Ionel, "Model predictive control of 5L-ANPC inverter fed coreless AFPM motor with mitigated cmv in electric aircraft propulsion," in *2024 IEEE Energy Conversion Congress and Exposition (ECCE)*. IEEE, 2024, pp. 2498–2505.

[17] J. F. Gieras, *Permanent magnet motor technology: design and applications*. CRC press, 2009.

[18] A. M. El-Refaie, "Fractional-slot concentrated-windings synchronous permanent magnet machines: Opportunities and challenges," *IEEE Transactions on industrial Electronics*, vol. 57, no. 1, pp. 107–121, 2009.

[19] M. Vatani, Y. Chulaee, J. F. Eastham, and D. M. Ionel, "Analytical and FE modeling for the design of coreless axial flux machines with Halbach array and surface PM rotors," in *2024 IEEE Energy Conversion Congress and Exposition (ECCE)*. IEEE, 2024, pp. 5205–5211.

[20] S. P. Colyer, P. Arumugam, and J. F. Eastham, "Modular airgap windings for linear permanent magnet machines," *IET Electric Power Applications*, vol. 12, no. 7, pp. 953–961, 2018.

[21] D. Talebi, M. C. Gardner, S. V. Sankarraman, A. Daniar, and H. A. Toliyat, "Electromagnetic design characterization of a dual rotor axial flux motor for electric aircraft," *IEEE Transactions on Industry Applications*, vol. 58, no. 6, pp. 7088–7098, 2022.